Electric Power Systems Research 247 (2025) 111788

Contents lists available at ScienceDirect

Electric Power Systems Research

journal homepage: www.elsevier.com/locate/epsr

Analysis of DC–DC converters as critical components for maritime DC grid simulation

Marlin Malpricht, Jana Ihrens, Thorsten A. Kern *

Hamburg University of Technology, Institute for Mechatronics in Mechanics, Eissendorfer Str. 38, Hamburg 21073, Germany

ARTICLE INFO

Keywords:
DC–DC converter
Maritime DC grids
Simulation complexity
Modeling
Power hardware-in-the-loop

ABSTRACT

The level of simulation detail accounts for system stability and dynamic response performance and is key to optimize between simulation accuracy and complexity. This study investigate its impact in shipboard DC grids focusing on power electronic converters as a critical component. A DC–DC forward converter model was analyzed with varying levels of complexity incorporating parasitic elements and compared to empirical data recorded at 100 kHz from a real DC–DC converter. The comparison was made regarding their time domain response to a load steps and their frequency domain characteristics. Results indicate that key characteristics like settling time and steady-state behavior can be accurately represented at moderate complexity, whereas capturing full system dynamics in time as well as frequency domain requires coupled hardware and digital simulations (Hardware-in-the-loop - HiL) due to component intricacies and parameter uncertainties.

1. Introduction

Due to the ongoing climate crisis, CO_2 emissions need to be lowered. By the use of heavy oil, the maritime sector is responsible for 2.5% of the global CO_2 emissions [1]. The European Union and the International Maritime Organization therefore emphasize the reduction of CO_2 emissions by 40% until the year 2030 [2]. To reach this goal, extensive changes need to take place, including technical improvements, emission trading and the use of regenerative energy sources [3,4]. Changes also need to be made not only to the way electrical power is generated, but also to how the generated power is transported throughout the ship. To make the most out of modern, environmentally friendly fuels, using DC grids on ships yields a more efficient use of the generated energy by minimizing conversion losses and operating generators at their optimal operating point. It also makes the addition of decentralized energy sources (DES) like photovoltaics (PV) or energy storage solutions (ESS) more efficient [5–7]. During the design phase of ships using DC grids, simulations need to be used, since building a prototype is often infeasible and there are not yet many ships using DC grids. Especially for larger ships, the transition to DC grids has not yet begun. In order to approximate the real world as close as possible, detailed models of DC grids need to be created and evaluated. With that comes a higher degree of complexity regarding building the model, run-time of the simulation itself and evaluating its results [8]. Highly complex simulation models make the development process impractical and inherit the risk of system oversizing. On the other hand, missing important details using a simplified simulation model might yield a higher risk of failure later in the design process or, at worst, during operation of the ship. As a result, there is a conflict between accuracy and complexity that needs to be balanced [9]. This works aims at solving this conflict by identifying critical components as a part of maritime DC grid simulations, that need to be simulated with a high level of detail (LoD) in order to achieve an accurate result. Non-critical components can be simulated with a lower LoD, thereby reducing simulation complexity. In Section 2, an exemplary DC grid of a ship is introduced, on the basis of which the most influential components of shipboard DC grids are presented and evaluated regarding their influence on system stability and complexity. In Section 3, a simplified and a complex model of a DC–DC converter is implemented in MATLAB® Simulink® and investigated in several scenarios. A measure of complexity is discussed and evaluated using aforementioned models. To verify the results, an experiment is performed in Section 4 using a real DC–DC converter, exposing it to scenarios resembling real world conditions onboard a ship and measuring its performance. The results of the experiment and the simulation are then compared in Section 5.

2. Identification of critical components

Shipboard energy systems are complex and unique by design. Every ship operates in a different environment, fulfills different tasks and therefore has different requirements regarding its energy generation

* Corresponding author.
E-mail addresses: marlin.malpricht@tuhh.de (M. Malpricht), jana.ihrens@tuhh.de (J. Ihrens), t.a.kern@tuhh.de (T.A. Kern).

https://doi.org/10.1016/j.epsr.2025.111788
Received 7 May 2024; Received in revised form 5 November 2024; Accepted 29 April 2025
Available online 30 May 2025

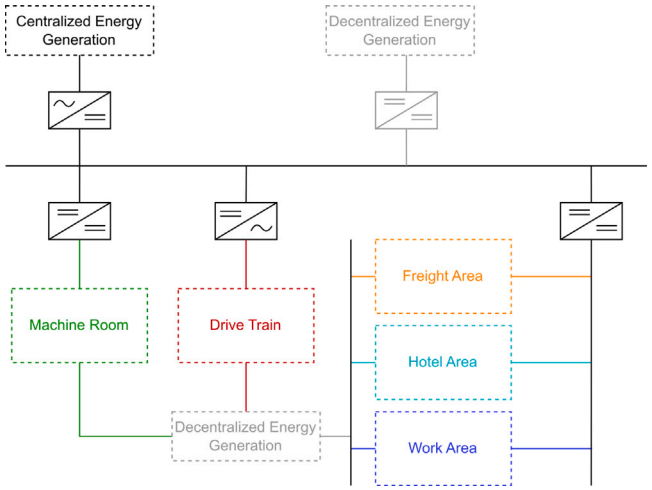

Fig. 1. Modularization of an exemplary shipboard energy system using DC, comprising different voltage levels and AC subsystems [4].

and distribution [4]. This makes the design phase of new ships using DC grids a challenging task. One approach to simplify the design and make DC grids more applicable to a wide variety of ships is the modularization and standardization of the energy system, as presented in [4]. Commonly used parts can be grouped together in modules and connected via standardized interfaces to fulfill most requirements of today's ships. An example of such modularization is shown in Fig. 1. In this section, components of a DC energy system on a ship will be investigated regarding their properties, expected loads and influence on the shipboard energy system.

2.1. Components of DC grids on ships

The overall architecture of a possible DC energy system of a ship is shown in Fig. 2.

The generators supply the main medium voltage DC (MVDC) bus via rectifiers. It supplies the main propulsion system via frequency converters as well as the low voltage DC (LVDC) system. The LVDC system supplies the engine room as well as other loads on the ship. On the MVDC or LVDC level, DES or ESS can be installed. The LVDC system also supplies the vertically arranged firezones.

The main components of the presented exemplary shipboard energy system can be grouped by functionality:

- Generation of electrical power: Generators are responsible for supplying most of the needed power during operation. The generated power is rectified and then connected to a DC bus. DES or ESS can be connected directly to either MVDC or LVDC bus, because of their inherent DC architecture.
- Motors and Propulsion: Propulsion system mostly rely on frequency controlled motors, that can be supplied by the MVDC bus. As they rely on AC, a frequency converter needs to be used. Additionally, several other motors and pumps for different purposes like heating, ventilation and air conditioning can be connected either directly or via a frequency converter, if needed.
- Switches and breakers: These are a very important part of shipboard energy systems, regardless of the use of DC or AC. They are an essential part of fulfilling security requirements and offering redundancy to critical parts of the ship. Due to the lack of a natural zero crossing in DC, circuits breakers and switches need to become more complex, as described in [10,11].
- Resistive loads: Most other electrical loads can be represented as purely resistive. These can range from lights, galley equipment and laundry to any other electrical device plugged into a low voltage outlet. Most of them only have a tiny impact on the load profile of the ship, but they are by far the largest group of consumers.

Due to the different architecture of shipboard DC grids in comparison to AC grids and their resulting converter driven dynamics, a more complex control architecture has to be implemented. The majority of DC shipboard energy systems are equipped with a control system that is structured into three distinct levels [5]. The lowest level, referred to as the primary level, is responsible for ensuring the fundamental functionality of the system, including current and voltage regulation through droop control, as well as the distribution of power. The secondary control level is tasked with maintaining the quality of power and managing power flow. The tertiary control level is primarily concerned with optimizing the system for economic and efficiency considerations. Converters and converter-to-converter communication play a crucial role in local primary control.

2.2. Selection of potential critical components

The goal of this work is to provide a guideline on which elements of a shipboard DC grid need to be modeled and simulated with a very high LoD in order to provide a realistic simulation output, while still keeping the simulation complexity and necessary resources as low as possible. In order to assess the criticality of the many aforementioned individual components in a maritime DC grid, several categories need to be considered.

- Influence on system stability: If the component has a high influence on system stability, an accurate representation of the behavior is desirable already in the design phase to ensure stable operation, a high level of power quality and compliance with all regulations.
- Contribution to system safety: A component responsible for dealing with fault scenarios or other safety related situations needs to be accurately defined and its functionality with all should be thoroughly understood.
- Number of occurrences inside the DC grid: One small deviation from reality of a simulation model can have great effects on the whole system if the component is installed in many places inside the ship.
- Power level of operation: Faults and misbehavior at high power levels can have much more impact on the energy system than low power components.
- Complexity of the component itself: If the component consists of multiple parts, that interact dynamically with each other, it is much more complex to design a model that behaves the same. This is exacerbated, if not all parameters of the real component are known during the design phase.

All components being part of a shipboard DC grid are listed and characterized in Table 1 based on the introduced categories.

Resistive loads are widely spread throughout the ship and range from lights, entertainment equipment to power supplies or outlets, usually operating in the watt to kilowatt range and having a very low level of complexity. As their load profile changes continuously during the day, modeling using white noise with a dynamically changing DC offset is possible. The only influence on system stability are big load spikes or drops generated by switching on or off multiple devices of this category at the same time.

Switches and solid-state circuit breakers (SSCBs) are an essential part of a DC energy system. They connect and fuse subsystems and therefore play an important role in system safety and redundancy. In addition, SSCBs are more complex than their AC counterparts because of higher short circuit current and no inherent zero crossing in

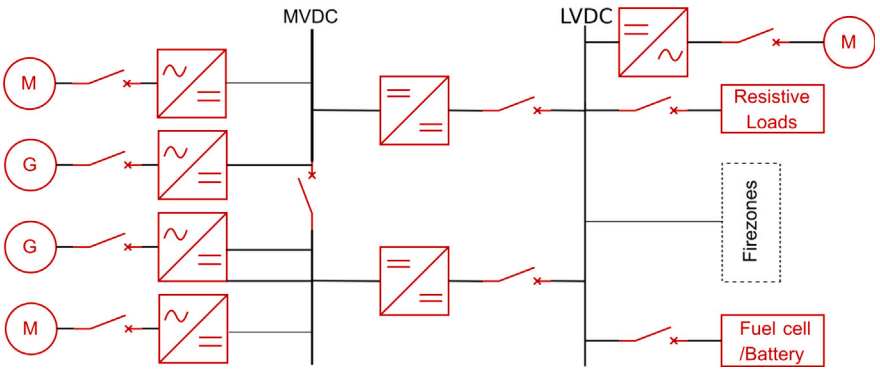

Fig. 2. DC Energy system architecture of an exemplary ship with two power levels — Medium Voltage DC (MVDC) and Low Voltage DC (LVDC) — including two main engines (M) and two generators (G), showing redundancy switching levels for distribution. Additionally, comprising an auxiliary motor (e.g., thruster) on the LVDC level and further power storage units.

Table 1
Overview of components in DC grids and their properties.

Component	Contribution to system stability	Contribution to electrical system safety	Number of occurrences	Power density	Complexity
Resistive loads	During load spikes/Drops	Low	Very High	W–kW	Low
Switches/Breakers	During switching operation	High	Medium	NA	Higher than in AC
Motors	High via Frequency converter	Low	Medium	kW–MW	High
Generators	High via Rectifier	Low	Low	MW	High
DC–DC converters	High	Low	High	W–MW	High

DC [6,11]. Nevertheless, for simulations not focusing on fault scenarios, breakers and SSCBs can simply be modeled by opened or closed switches and therefore are not considered in this work.

Motors are very commonly used on ships, not only for propulsion, but also for pumps and in HVAC systems. They are present at multiple different voltage levels and can operate at up to several kilowatts or, in case of the propulsion system, up to megawatts. While DC motors can be directly connected to the proposed DC grid, variable frequency converters drive all other motors. Their high power consumption and their variable frequency operation can yield a high influence on system stability if voltage ripples are injected into the DC system via the frequency converters and thereby reduce the quality of service (QOS).

With DC grids, generators can provide electrical power much more efficiently as they are no longer fixed to one specific frequency [6]. Their high power output and independent operating frequency, if used with frequency converters, combined with the dynamics of the downstream rectifiers makes them a candidate for inducing oscillations into the DC system. Because of the large complexity and uniqueness of such generators, due to the interaction of chemical, mechanical and electrical energy, it is infeasible to build a highly accurate simulation model. The research should therefore focus on the precise modeling of the rectifiers downstream, that can then be validated and reinforced using real world measurements and power hardware-in-the-loop (PHiL) simulations [12].

Converters are one of the most essential parts of a shipboard DC grid. Not only do they operate at a higher voltage than their terrestrial or aerospace counterparts, but reliability and safety on ships has a high priority [13]. Most of the interfacing and connection of the different subsystems with loads and power generation is done via converters. That is why, as can be seen from Fig. 2, there are many converters present in a shipboard DC grid. They also have a high influence on system stability, as their high frequency operation and switching may induce voltage ripples on either side of the interfaced system. The effects are intensified when many converters are used in parallel [11,14]. In addition to that, converters are a very complex component due to their many parts, active elements, high switching frequency and mostly software based control architecture [15].

Concluding this evaluation, it can be stated that, from a theoretical point of view, power electronic converters are the most critical component onboard a DC grid due to their interfacing utilization, complex architecture, software based control as well as their high influence on system stability and QOS. Therefore, a detailed comparison between simulation complexity and accuracy of DC–DC converters will be pursued in the following sections.

3. Simulation of a DC-DC converter

The accurate simulation of system dynamics without incurring excessive computational effort is a critical issue that has rarely been addressed [16]. In this section, a DC–DC converter model is introduced and simulated with different complexity levels to systematically analyze the influence of the LoD. Model characteristics are evaluated in time domain as well as in frequency domain. The time domain analysis is performed in order to gain an understanding of how different complexity levels of the model influence the system response to an exemplary load step and how good the simulated response fits the real world data measured in Section 4. This is crucial to comprehend the system's behavior in response to a load step, e.g., the settling time or peak overshoots that could influence system stability, in order to gain a comprehensive understanding of its functioning. The frequency domain analysis is important to assess how voltage ripples on either side of the converter could influence or interfere with the whole energy system. Voltage ripples can appear even in DC grids because of its converter dominated architecture [17]. It is therefore desirable to get an understanding on how different harmonics, either from motors, generators or from the converters themselves, propagate through the grid and where resonant frequencies may cause instabilities. To investigate on how different complexity levels of the simulation model influence the results, the model complexity is modified by including parasitic elements into the model. Multiple sensitivity analysis are performed to assess how different model parameters affect the result and to determine the needed LoD for a viable simulation result.

3.1. DC–DC converter model

The converter being used in Section 4 is a 480 W Wago prototype converter. Therefore, a forward converter model [18] has been implemented in MATLAB® Simulink® using the "Specialized Power Systems" environment. The resulting simulation model is shown in Fig. 3.

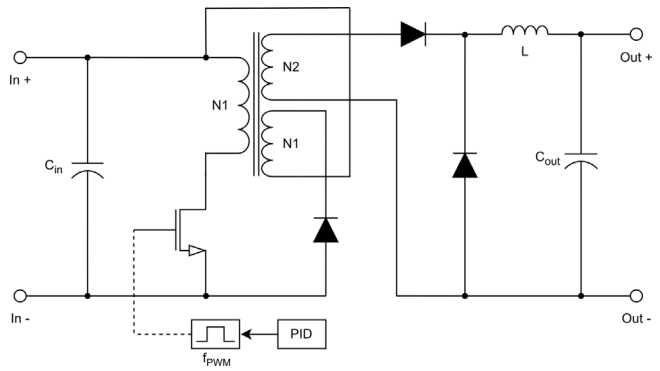

Fig. 3. DC–DC converter simulation model in forward converting architecture for comparison between the simulation model and HIL behavior.

Table 2
Simulation model parameters.

Parameter	Value
Input voltage U_{in}	350 V
Output voltage U_{out}	24 V
Power P	480 W
Transistor on-time $t_{on,max}$	0.5
Controller P	2
Controller I	200
Controller D	0
Controller Frequency f_{pwm}	100 kHz
Input capacitance C_{in}	150 mF
Output capacitance C_{out}	100 µF
Inductance L	0.045 mH
Primary windings N	794
Secondary windings $N2$	109
Magnetization Inductance L_m	100 mH

The main characteristics of a forward converter are the galvanic isolation and the two primary windings $N1$ with the same polarity. Knowing the desired input and output voltage as well as the power density, eleven more design parameters need to be set. The parameters and their selected values for the used model are listed in Table 2. The PWM frequency f_{pwm} of the controller has been set to 100 kHz and the output inductance L has been calculated with the desired output voltage V_{out} and the maximum power P of the converter.

$$L = \frac{V_{out}^2}{0.4 * P * f_{pwm}} \tag{1}$$

The number of secondary windings $N2$ has been calculated using the input voltage V_{in}, output voltage V_{out} and the maximum on-time of the transistor $t_{on,max}$ with

$$N2 = N1 * \frac{V_{out}}{V_{in}} * \frac{1}{t_{on,max}} \tag{2}$$

According to [18,19]. The maximum duration the transistor can be on per one duty cycle $t_{on,max}$ is set to 0.5 in order to ensure full demagnetization of the second primary coil [18].

Tweaking of the design parameters has been performed using a sensitivity analysis investigating the influence of certain components and their values on the variance of the input current and the output voltage. The results are shown in Fig. 4. They show that there is a strong dependency between the input current variance and the input capacitance, as well as between the output voltage variance and the inductance. The output capacitance and the number of primary windings are not directly correlated with any of the investigated quantities, but moreover dependent on the relation and combination of the other parameters. Based on this analysis, the value of the inductance has been chosen as 0.045 mH instead of the calculated 0.03 mH and the number of primary windings has been chosen as 794. The model has been discreetly solved using the Tustin/Backward Euler solver with a sample time of 1 µs in order to have a similar sample time as the measurements taken in Section 4.

3.2. Model complexity

Simulation complexity and LoD are critical aspects that determine the effectiveness and applicability of simulation models in engineering systems. Simulation complexity refers to the measure of resources required to develop, run, and analyze a simulation model. It includes both computational complexity, which affects the execution time and computational resources, and structural complexity, which influences the model's development and comprehension as well as the subsequent analysis of results [20]. LoD, on the other hand, refers to the granularity of the model's representation of the real system. A model should only have as high a LoD as is necessary for the intended application, balancing the need for detail against the risks of increased error [21,22]. A lower LoD can lead to greater transparency and reduced error propagation, improving understanding and ease of use, though possibly at the detriment of precision [23]. The complexity of a simulation model can therefore be split into three categories mentioned in [8]:

- The time and information it takes to build the model
- The time and resources it takes to run the simulation itself
- The time and knowledge it takes to understand and evaluate the results

For the analyzed DC–DC converter, the model complexity is increased by taking parasitic components and parameters into account during model building and simulation. These parasitic elements do not increase the number of output quantities, therefore no additional knowledge or time is needed to interpret the results. Hence, the quantification of complexity in this work is based on the model parameters that need to be set or calculated and the time it takes to run the simulation of one or multiple instances of the same model. Structural complexity metrics, such as cyclomatic complexity [9], are not considered as it requires deep information of the underlying functions on which the modeled components are implemented. In order to include parasitic parameters, several components need to be extended. The extended models are shown in Fig. 5. The capacitance model is refined by adding a resistor and an inductor in series, as described in [24]. The parasitic capacitances between gate, drain and source of the MOSFET are added as described in [25]. Lastly, a parallel capacitance and a series resistor are added to the inductance [26]. Furthermore, additional parameters already included in the used components have been activated. All parameters of the complex model and their respective values are listed in Table 3

Including parasitic elements, the total number of simulation parameters rises to 28, doubling the 14 parameters needed for the simplified simulation. If the two capacitors and the three diodes are treated independently, the number of parameters reaches 38. In addition to the increased number of parameters, it is severely more difficult to estimate, or even calculate the parasitic parameters of components like capacitors, inductances or MOSFETs. This is because these parameters are mostly component specific and often dependent on factors like power density or operating temperature. Therefore, sensible base values have been selected and their effect on the input and output quantities over a broad range of values has been investigated using another sensitivity analysis. The value range is also mentioned in Table 3. The resulting tornado plots are depicted in Fig. 6. These show that only some parasitic values have a direct correlation to one of the output quantities. The diode capacitance has a high influence on the input current mean and variance, whereas the MOSFET capacitances mostly affect the input current mean. The series resistance of the capacitor however has a very high influence on the input current variance only. At the output, the series resistance of the inductor, the diode forward voltage and on-resistance of the diode as well as the winding resistance

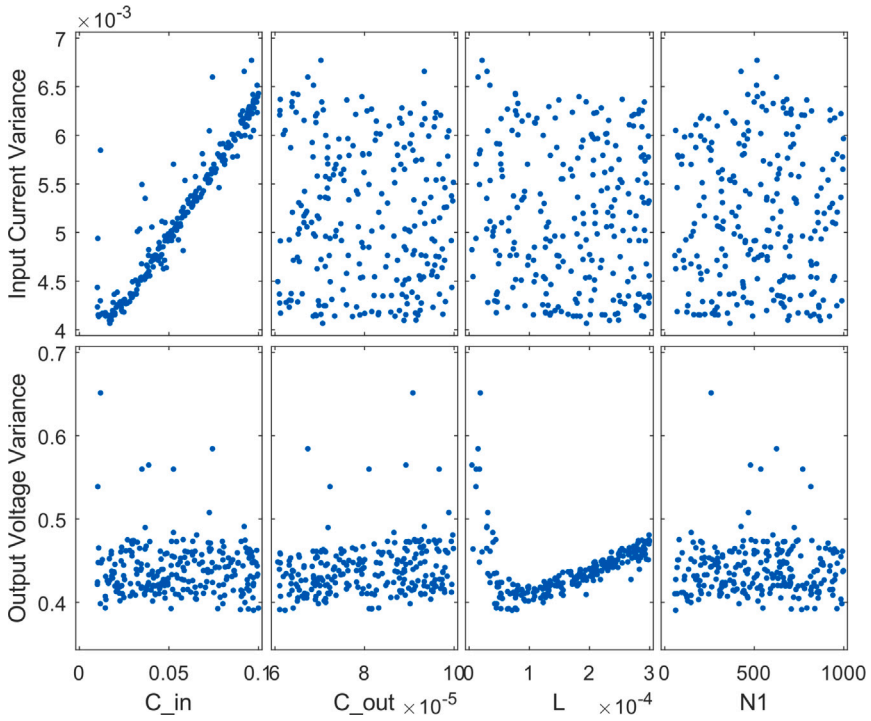

Fig. 4. Sensitivity analysis of the design parameters for the forward converter simulation model, showing high sensitivity of the input current to input capacitance and output voltage to the inductance.

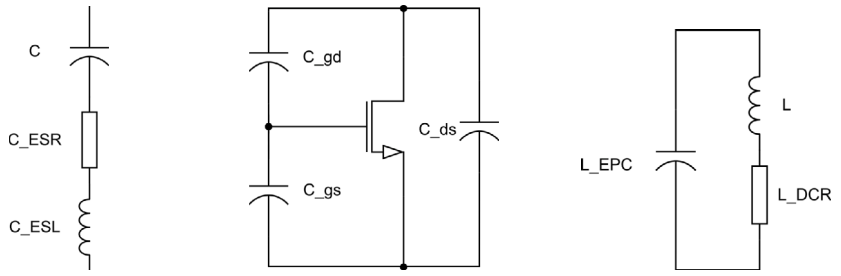

(a) Capacitor [24] (b) MOSFET [25] (c) Inductor [26]

Fig. 5. Extended component models with parasitic elements.

of the transformer have the highest correlation with the output voltage dynamics. The other parameters do not have a strong correlation to any of the output quantities. Instead, only the combination of them result in one specific outcome of the simulation, leading to an even more complex model building process.

To evaluate the model complexity regarding the simulation run-time and resources, the model has been executed with up to nine DC–DC converters in parallel ten times each. For each run, the execution time is measured, later an average is calculated. The results are then compared between the simplified and complex simulation model. Because the fluctuation of computation time is not normally distributed, the Mann–Whitney U-test is used to evaluate the statistical difference between the measured simulation times [9,27]. The results in Fig. 7 show not only the exponential rise of the simulation time the more parallel converters are added, but also that the difference between the simulation time of the simplified and complex model increases linearly. For one simulated converter, the simulation time of the simplified and complex simulation model is almost the same. With seven parallel converters, the average simulation time of the complex model is almost twice as long as of the simplified model. This further underlines the goal of this work, generating an efficient and still valid simulation of a shipboard DC grid in order to reduce simulation run-time. Executing the Mann–Whitney U-test shows that the difference between the simulation times is significant for each of the performed simulations. The results from the simulation models of different complexity are evaluated and compared to a real DC–DC converter in Section 5.

4. Experiment

For real world data and validation, a DC–DC converter has been analyzed in the Power Hardware-in-the-Loop Laboratory (PHiLsLab) at TUHH, briefly introduced in [4,12]. In order to assess the validity of the simulation results and the dependency on model complexity, the characteristics of the converter are investigated in four different categories:

- Time domain response to a load step (Fig. 8(a))
- Frequency domain characteristics of the converter during steady-state operation (Fig. 8(b))
- Frequency domain response to voltage ripples of different frequencies on the primary side of the converter (Fig. 8(c))
- Frequency domain response to voltage ripples of different frequencies on the secondary side of the converter (Fig. 8(d))

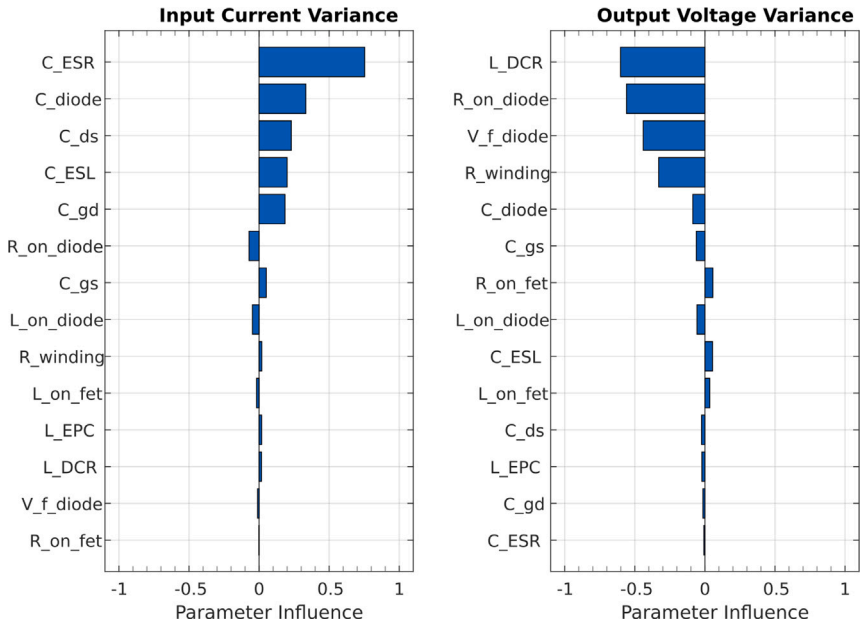

Fig. 6. Correlation between parasitic component parameters and measured output quantities, showing high correlation for parasitic capacitances with input currents and inductor series resistance, diode on-resistance, diode forward voltage, and winding resistance with output voltage.

Table 3
Complex simulation model parameters.

Parameter	Value	Value range
Diode		
On-Resistance R_{on}	10 mΩ	10–100 mΩ
On Inductance L_{on}	5 nH	5–50 nH
Forward Voltage V_f	0.3 V	0–1 V
Capacitance C_{diode}	10 pF	10–1000 pF
Inductor		
Parallel Capacitance L_{EPC}	50 nF	10–90 nF
Series Resistance L_{DCR}	10 mΩ	10–100 mΩ
Capacitor		
Series Inductance C_{ESL}	1 nH	1–10 nH
Serial Resistance C_{ESR}	1 mΩ	1–20 mΩ
MOSFET		
On-Resistance R_{on}	1 mΩ	1–100 mΩ
On Inductance L_{on}	5 nH	5–100 nH
Drain Source Capacitance C_{ds}	10 pF	10–1000 pF
Drain Gate Capacitance C_{gd}	10 nF	10–1000 pF
Gate Source Capacitance C_{gs}	1 nF	1–3 nF
Transformer		
Winding Resistance $R_{winding}$	50 mΩ	10–100 mΩ

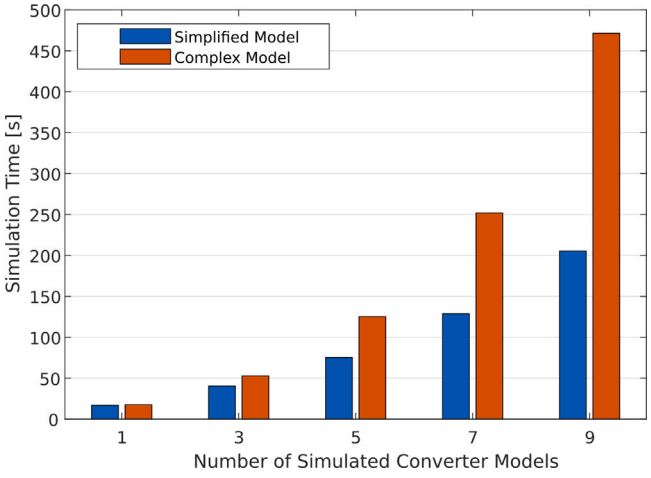

Fig. 7. Averaged simulation run-time with multiple parallel converters, illustrating a linear increase in time difference between simplified and complex models.

The time domain analysis has been performed by connecting the primary side of the DC–DC converter to a bidirectional DC power source by *Elektro-Automatik*, model number *PBS11500-604U*, supplying the converter with 350 VDC. The secondary side has been connected to a second bidirectional DC power source of the same model, operating in sink mode. The measurements have been taken with a precision power analyzer by *ZES Zimmer* with the model number *LMG671*. The input and output current and voltage were measured with a sample rate of 606.061 kS/s. The current sink has been programmed to simulate a load step from 10 % to 90 % i.e., 2 A to 18 A and vice versa. The frequency domain characteristics of the converter during steady-state operation can only be obtained on the secondary side of the converter as, on the primary side, the voltage supply characteristics are always included in the measurement. Therefore, the primary side cannot be investigated independently. To measure the output characteristics of the converter during steady-state operation, the secondary side has been connected to a 12 Ω passive power resistor. For the dynamic frequency domain analysis, the goal was to simulate low voltage AC ripples with variable frequency superimposed on the nominal DC voltage. Therefore, a four quadrant AC amplifier by *Spitzenberger & Spies* with the model number *APS A6310*, capable of outputting a DC voltage as well as combining it with an AC ripple of up to 100 kHz has been used. To analyze the effect of harmonics at the primary side of the converter, the DC voltage was set to 300 V and an AC chirp signal spanning from 1 Hz to 100 kHz with a resolution of 1 Hz and an amplitude of 1 V has been added. Each frequency step has been held for at least ten periods of the respective frequency. The load was again represented by the DC sink operating at 50 % load, i.e., 10 A. Investigation of backward coupling from the secondary side to the primary side of the converter has been done by connecting the AC amplifier to the secondary side of the converter and operating it in current sink mode. AC ripples with the same frequency as previously mentioned and an amplitude of 500 mA have been added to the DC offset of 10 A. The converter was again supplied by the bidirectional DC power source.

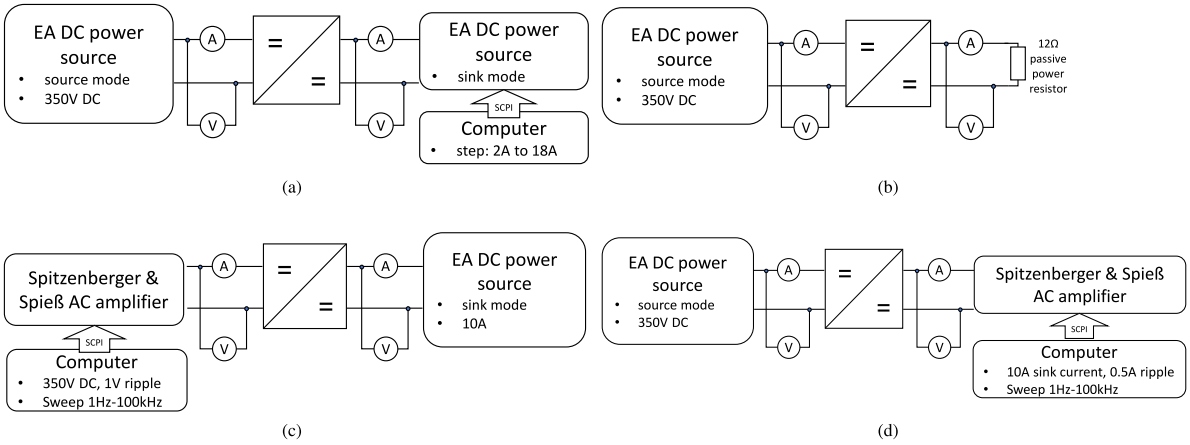

Fig. 8. Experimental setups for DC–DC converter analysis: (a) Time-domain response to a load step with fixed 350 V DC supply (b) Frequency-domain analysis of the converter in steady-state operation with fixed 350 V DC supply and a passive resistor (c) Frequency-domain response to voltage ripples on the primary side with a 350 V DC supply and constant current output (d) Frequency-domain response to current ripples on the secondary side with 10 A and fixed 350 V DC supply.

5. Comparison of the results

In this section, simulation results with and without parasitic elements are compared to each other as well as to the real world component measured in the aforementioned scenarios.

5.1. Time domain load step

To assess the time domain characteristics of the simulation and the real converter, a load step has been applied and the resulting input and output current as well as the output voltage have been monitored. The input voltage is not captured because it is held stable by the connected voltage source, and therefore does not offer much insight into the dynamics of the converter. Two load steps have been applied to investigate the different behavior during a sudden load rise or drop. The results are shown in Fig. 9. For better visualization, the abscissa is scaled differently on the input and output measurements.

A comparison of the model and experimental dynamics reveals discrepancies in their exact dynamics. Nevertheless, the settling time of the measured quantities are comparable. Furthermore, the complex model can be used to represent the voltage drop at the output. The exact value of the resulting output voltage under load is dependent upon the precise values of the components, and thus differs from the experimental results. Furthermore, the simulated output current waveform in Fig. 9(a) exhibits similar characteristics to the measured one, specifically a first peak followed by a decline in current, which is then followed by a larger peak. In contrast, these dynamics are not reflected in the simulation of a load drop depicted in Fig. 9(b). The discrepancy between the simulation and reality is most apparent in the output voltage peaks. With the rising load step in Fig. 9(a), the simulated voltage drops to 16 V while the measured voltage stays above 21 V. During the load drop in Fig. 9(b), the simulated voltage rises to 30 V or 33 V, respectively, while the measured voltage only reaches 24.5 V. The absence of these peaks in the real DC–DC converter can be attributed to the presence of built-in protection circuitry, which serves to prevent damage to the connected load by maintaining a stable output voltage. Fig. 9(b) also illustrates a notable negative current flowing back into the converter following the removal of the load. This discrepancy may be attributed to the internal configuration of the current sink, which may not fully align with the converter's intrinsic characteristics. The pronounced fluctuations observed in the measured input current in Fig. 9(b) are, however, intrinsic to the converter and are likely attributable to the converter's internal control algorithm. Consequently, these dynamics are not amenable to reproduction through simulation using the same component.

5.2. Frequency domain characteristics during steady-state operation

As described in Section 4, the steady-state characteristics can only be analyzed for the secondary side of the converter, because the primary side characteristics would be dominated by the connected voltage supply. To achieve the results shown in Fig. 10, a 12 Ω resistor was connected to the output of the converter in order to only measure the converter and not any actively controlled current sinks. The results demonstrate, that the output characteristic of the converter is predominantly flat, whereas the simulation starts with a higher gain at low frequencies but then drops after 1 Hz. While both the simulation and the measured data are not similar, neither exhibits any notable characteristics. The simulation results have a peak at 100 kHz, being the PWM frequency of the controller, and a dynamic behavior between 1 kHz and 20 kHz. With the exception of a higher drop-off at frequencies exceeding 20 kHz of the simplified simulation model, both simulation models have the comparable characteristics. The absence of any peaks in the measured converter output may be attributed to the presence of advanced filter circuitry, which serves to ensure stable and resonant-free operation of the connected load.

5.3. Frequency response to primary side voltage ripples

To analyze the effects of harmonic distortions on the DC bus connected to the primary side of a DC–DC converter, the DC input voltage has been superimposed with an AC ripple of variable frequency ranging from 1 Hz to 100 kHz. As both the primary and secondary side of the converter are connected to active sources and sinks respectively, it is important to note that the results not only show the characteristics of the investigated converter but also of the voltage supply and current sink. From the results in Fig. 11 it is apparent that there are two resonant frequencies present that manifest with a high gain of the input current. They are located around 7 kHz as well as 20 kHz. They do, however, not appear at the output of the converter. Only low frequency harmonics up to 10 Hz are also visible at the secondary side of the converter. At low frequencies, the internal controller tries to counteract the fluctuating voltage at the input, resulting in visible fluctuations at the output. These harmonics can also be seen in the simulation results, proving a similar behavior at those frequencies. At higher frequencies, both the simulation model and the real converter behave similarly, lacking any characteristic peaks. The two peaks at 20 kHz and 40 kHz in the output voltage and current are caused by the used current sink. Comparing the simplified and complex simulation models, they follow the same trend, but the complex model with parasitic elements has fewer dynamics than the simplified model.

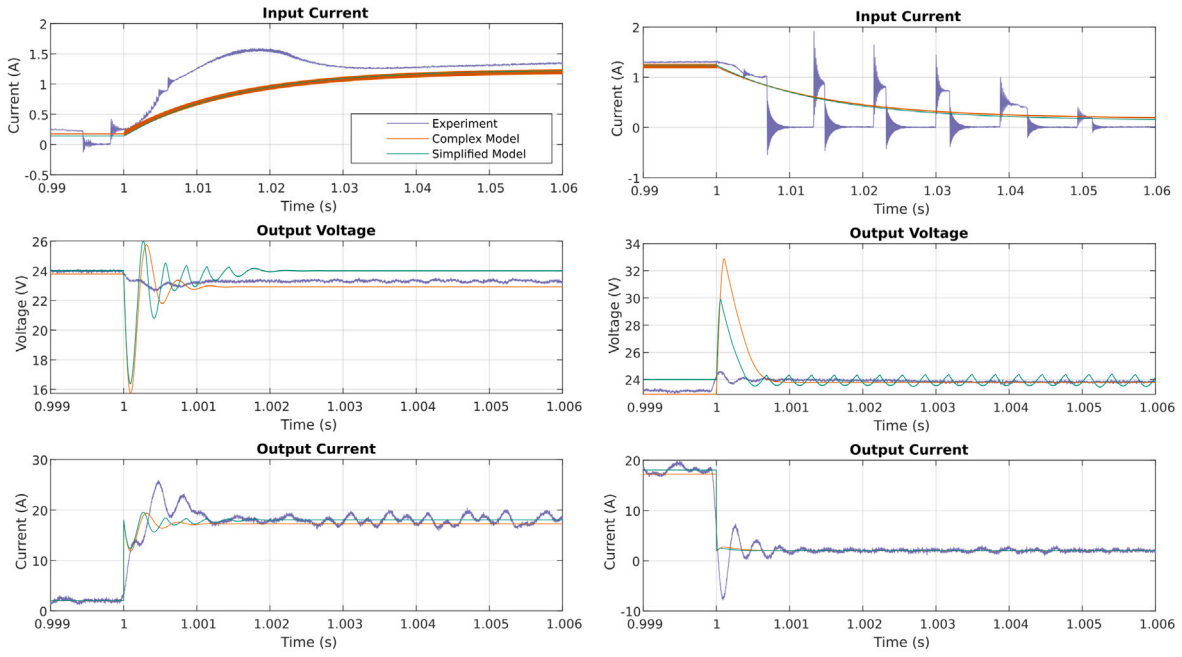

Fig. 9. Time domain response to a load step of the simulation model with different LoD and the real converter showing comparable results for settling time and steady-state behavior: (a) 10% load to 90% load (b) 90% load to 10% load.

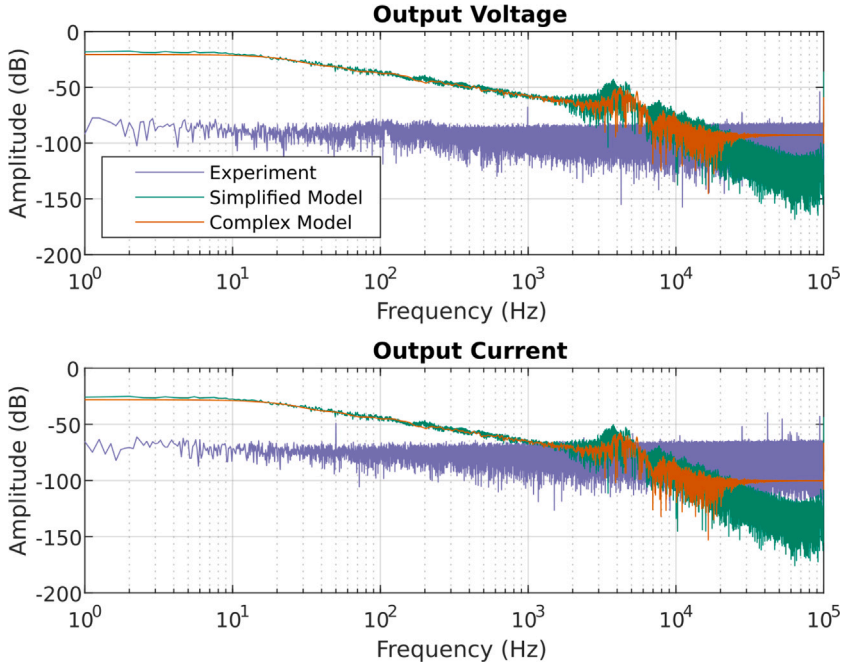

Fig. 10. FFT of the output voltage and current during steady-state operation, depicting a mostly flat characteristic of the real converter in comparison to the simulation model.

5.4. Frequency response to secondary side current ripples

Investigating the effects of harmonics at the secondary side of the converter is important to verify if any backward coupling from the secondary to the primary side is present, possibly interfering or distorting the QOS on the primary side DC bus. Fig. 12 shows that, specifically, the low frequency harmonics can propagate through the converter to the primary side, whereas frequencies upward of 100 Hz do not have any significant impact at the primary side of the converter.

There are however some dynamics at the output voltage attributable to resonant frequencies, e.g., at 2.5 kHz. These are present in the simulation as well as in the measured data from the real converter, but at different locations. Resonant frequencies are highly dependent on the internal components and their parameters, and therefore hard to include into a simulation model. The results also show that the frequency response of the simulation is again similar to the one of the real converter, except for the aforementioned resonant frequencies.

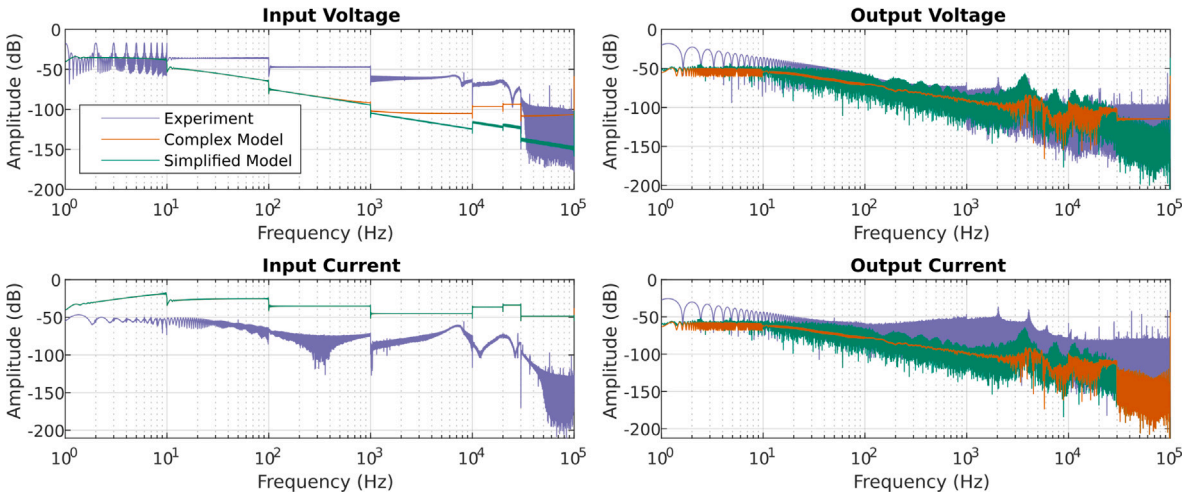

Fig. 11. Frequency response of the converter to harmonic voltage ripples of 1 V at 1 Hz to 100 kHz at the input, indicating only low frequencies at the input are transmitted to the output. Additionally, resonant frequencies can be observed at 7 and 20 kHz.

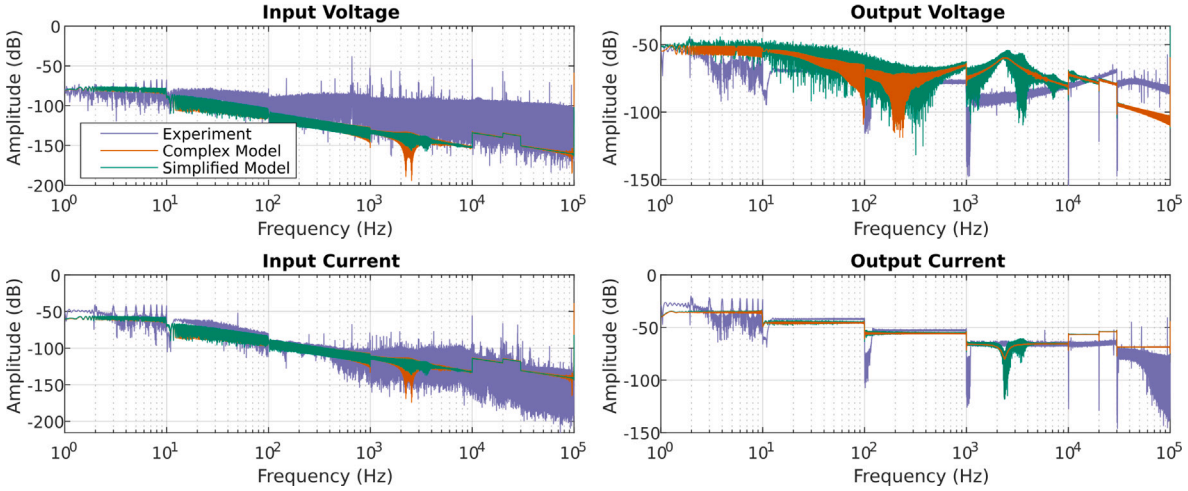

Fig. 12. Frequency response of the converter to harmonic current ripples of 500 mA at 1 Hz to 100 kHz at the output, highlighting resonant frequencies at the output and propagation of low frequencies to the primary side.

5.5. Interpretation of the results

Summarizing the presented results, it can be stated that a simulation model can represent the dynamic behavior of a DC–DC converter within certain limits. Time domain behavior like settling times can be accurately simulated even with a simplified simulation model without any parasitic components. However, the simulation model, regardless its complexity, was not able to accurately represent current or voltage peaks during load steps. During these scenarios, the software control algorithm has a significant impact on the dynamic behavior. The same applies for the frequency domain characteristics. As these are influenced by many internal components and their relation to each other, it was not possible to recreate the real behavior with the simulation. However, the results demonstrate, that there is no forward or backward coupling between the input and output of the converter if harmonic distortions are present and that this can even be accurately represented with a simulation model of low complexity. This emphasizes the criticality of power electronic converters in DC grid simulations, as their interfacing architecture requires the system designer to know, how different dynamics at the ports of the converter propagate through to the other side. Knowing this can help simplify simulations of the whole shipboard DC grid by splitting up the model at the converter and running multiple partial simulations in parallel. Another approach based on these findings can be the more extensive simplification of the simulation model, replacing the converter with a faster, less complex model as presented in [15].

6. Conclusion

In this work, the upcoming challenges of accurately representing shipboard DC grids in a simulation model are presented. To tackle these challenges and find a balance between simulation complexity and accuracy, critical elements in DC grids are identified. Knowing these critical components can help to focus the simulation model complexity to some components, while simplifying other, non-critical components. During the design phase, when no prototype is available, performant but still accurate simulation models are crucial to minimize risks and limit system oversizing. Since shipboard DC grids are converter dominated [17], it has to be ensured that their dynamics are represented as detailed as possible. Because of their interfacing architecture, inherent complexity and high influence on system stability, power electronic converters are identified as a critical component inside DC grids. To prove this, a simulation model of different complexity and a real world DC–DC converter are compared regarding their dynamic behavior. The results show, that converters have a high influence on the general simulation complexity and computation time, as well as on the dynamic

behavior of the resulting system. Further, it is demonstrated that system parameters like the settling time and steady-state behavior can be accurately represented even with simple models. However, to gain information about full system dynamics in time as well as frequency domain, HiL simulations contribute significantly to the quality of the predictions due to uncertain parameter values and component intricacies. Knowing this can help build future DC grid simulation models, simplifying non-critical components while keeping simulation accuracy high and model complexity low.

CRediT authorship contribution statement

Marlin Malpricht: Writing – original draft, Visualization, Methodology, Investigation, Formal analysis, Data curation, Conceptualization. **Jana Ihrens:** Writing – review & editing, Writing – original draft, Project administration, Methodology, Data curation, Conceptualization. **Thorsten A. Kern:** Writing – review & editing, Supervision, Resources, Project administration, Funding acquisition.

Funding

We gratefully acknowledge financial support through the Projektträger Jülich (PTJ) with funds provided by the Federal Ministry for Economic Affairs and Climate Action (BMWK) due to an enactment of the German Bundestag under Grant No. 03SX527D (SuSy).

Declaration of competing interest

The authors declare the following financial interests/personal relationships which may be considered as potential competing interests: Thorsten A. Kern reports financial support was provided by Federal Ministry for Economic Affairs and Climate Action (BMWK).

Data availability

The authors do not have permission to share data.

References

[1] MEP, MEPs call for a cleaner maritime transport, 2021, URL https://www.europarl.europa.eu/news/en/press-room/20210422IPR02632/meps-call-for-a-cleaner-maritime-transport. (Online Available Accessed 03 May 2024).

[2] IMO, IMO's work to cut GHG emissions from ships, 2023, URL https://www.imo.org/en/MediaCentre/HotTopics/Pages/Cutting-GHG-emissions.aspx. (Online Available Accessed 03 May 2024).

[3] MEP, Cutting emissions from planes and ships: EU actions explained|News|European Parliament, 2022, URL https://www.europarl.europa.eu/news/en/headlines/society/20220610STO32720/cutting-emissions-from-planes-and-ships-eu-actions-explained. (Online Available Accessed 03 May 2024).

[4] T.S. Hartwich, K. Sommer, T.A. Kern, L. Haffner, DC-Netze : ein ganzheitlicher systementwurf für verschiedene schiffstypen, 2023, http://dx.doi.org/10.15480/882.4392.

[5] Z. Jin, M. Savaghebi, J.C. Vasquez, L. Meng, J.M. Guerrero, Maritime DC microgrids - a combination of microgrid technologies and maritime onboard power system for future ships, in: 2016 IEEE 8th International Power Electronics and Motion Control Conference (IPEMC-ECCE Asia), 2016, pp. 179–184.

[6] R. Prenc, A. Cuculić, I. Baumgartner, Advantages of using a DC power system on board ship, J. Marit. Transp. Sci. 52 (1) (2016) 83–97.

[7] G.T.T. Vieira, M.B.C. Salles, R.M. Monaro, B.S. Carmo, 7th International Conference on Clean Electrical Power: Renewable Energy Resources Impact: Otranto, 2-4 July 2019, IEEE, Piscataway, NJ, 2019, http://dx.doi.org/10.1109/ICCEP46073.2019.

[8] R.J. Brooks, A.M. Tobias, Choosing the best model: Level of detail, complexity, and model performance, 1996, http://dx.doi.org/10.1016/0895-7177(96)00103-3.

[9] J. Ihrens, T. Schneider, T.A. Kern, Assessing the complexity of DC-system simulations, in: 2022 IEEE Workshop on Complexity in Engineering, COMPENG, IEEE, 2022, pp. 1–4, http://dx.doi.org/10.1109/COMPENG50184.2022.9905428.

[10] ABB, The step forward - Onboard DC grid, 2014, URL https://new.abb.com/docs/librariesprovider91/articles/lm00614-onboard-dc-grid-brochure_june2014_1.pdf. (Online Available Accessed 03 May 2024).

[11] K. Kim, K. Park, G. Roh, K. Chun, DC-grid system for ships: a study of benefits and technical considerations, J. Int. Marit. Saf. Environ. Aff. Shipp. 2 (1) (2018) 1–12.

[12] J. Ihrens, S. Möws, L. Wilkening, T.A. Kern, C. Becker, The impact of time delays for power hardware-in-the-loop investigations, Energies 14 (11) (2021) 3154.

[13] L. Xu, J. Guerrero, A. Lashab, B. Wei, N. Bazmohammadi, J. Vasquez, A. Abusorrah, A review of DC shipboard microgrids—Part I: Power architectures, energy storage, and power converters, IEEE Trans. Power Electron. 37 (5) (2022) 5155–5172.

[14] S. Jayasinghe, L. Meegahapola, N. Fernando, Z. Jin, J. Guerrero, Review of ship microgrids: System architectures, storage technologies and power quality aspects, Inventions 2 (1) (2017) 4.

[15] J. Ge, X. Huang, H. Xie, Fast equivalent model of isolated bidirectional DC-DC converters for DC microgrid study, in: IECON 2015 - 41st Annual Conference of the IEEE Industrial Electronics Society, IEEE, 2015, pp. 000031–000035, http://dx.doi.org/10.1109/IECON.2015.7392960.

[16] W. Zhu, J. Shi, S. Abdelwahed, End-to-end system level modeling and simulation for medium-voltage DC electric ship power systems, Int. J. Nav. Archit. Ocean. Eng. 10 (1) (2018) 37–47.

[17] R. Bartelt, D. Meyer, C. Heising, Y. Khimchenko, V. Staudt, Simulation of large-scale electric-ship DC-grids using the simulation tool VIAvento, in: 2013 IEEE Electric Ship Technologies Symposium, ESTS, IEEE, 2013, pp. 269–274, http://dx.doi.org/10.1109/ESTS.2013.6523745.

[18] R. Kories, H. Schmidt-Walter, Taschenbuch der Elektrotechnik: Grundlagen und Elektronik, 11., überarbeitete auflage ed., in: Europa Lehrmittel, Verlag Europa-Lehrmittel Nourney Vollmer GmbH & Co. KG, Haan-Gruiten, 2017.

[19] U. Schlienz, Schaltnetzteile und ihre Peripherie: Dimensionierung, Einsatz, EMV, 7., überarbeitete und erweiterte auflage ed., Springer Vieweg, Wiesbaden and Hei delberg, 2020.

[20] L. Chwif, M. Barretto, R.J. Paul, On simulation model complexity, in: 2000 Winter Simulation Conference Proceedings (Cat. No.00CH37165), IEEE, 2000, pp. 449–455, http://dx.doi.org/10.1109/WSC.2000.899751.

[21] D. Abel, A. Bollig, Rapid Control Prototyping: Methoden und Anwendungen ; Mit 16 Tabellen, 1. aufl. ed., Springer, Berlin and Heidelberg, 2006.

[22] C.A. Aumann, A methodology for developing simulation models of complex systems, Ecol. Model. 202 (3–4) (2007) 385–396.

[23] L. Kotzur, L. Nolting, M. Hoffmann, T. Groß, A. Smolenko, J. Priesmann, H. Büsing, R. Beer, F. Kullmann, B. Singh, A. Praktiknjo, D. Stolten, M. Robinius, A modeler's guide to handle complexity in energy systems optimization, Adv. Appl. Energy 4 (2021) 100063.

[24] R. Keim, Parasitic inductance, 2023, URL https://eepower.com/capacitor-guide/fundamentals/parasitic-inductance/#. (Online Available; Accessed 03 May 2024).

[25] Toshiba Electronic Devices & Storage Corporation, Power MOSFET electrical characteristics application note AKX00063-3, 2023, URL https://toshiba.semicon-storage.com/info/application_note_en_20230209_AKX00063.pdf?did=13415. (Online Available Accessed 03 May 2024).

[26] A. Alshaabani, B. Wang, Parasitic capacitance cancellation technique by using mutual inductance and magnetic coupling, in: IECON 2019 - 45th Annual Conference of the IEEE Industrial Electronics Society, IEEE, 2019, pp. 1928–1931, http://dx.doi.org/10.1109/IECON.2019.8927137.

[27] J. Bortz, G.A. Lienert, Verteilungsfreie Methoden in der Biostatistik: Mit 247 Tabellen, 3., korrigierte Aufl., in: Springer-Lehrbuch Bachelor, Master, Springer Medizin Verl., Heidelberg, 2008.